

Assessment of flow-induced vibration in radial gates during extreme flood

Karen Riddette and David Ho

WorleyParsons Services Pty Ltd

Recent dam safety reviews of a number of Australian dams have identified that the arms of raised radial gates may be partially submerged by extreme flows which exceed the original design flood for the dam. Various design solutions have been proposed to secure and strengthen the radial gates, however an important concern is the potential for flow-induced vibration. Under extreme flood conditions, flows near the gate arms will be high-velocity, free-surface, with a steep angle of attack on the arm beams. Traditional hand calculations for computing vibrations are of limited applicability in this situation, and there is little published data available for this combination of flow conditions and arm geometry. A detailed study using CFD modelling of the potential for vibration around radial gate arms was carried out for Wyangala Dam. This paper presents the results of the validation and reveals some interesting flow patterns and vortex shedding behaviour.

Keywords: flow-induced vibration, radial gates, CFD, Wyangala Dam, vortex shedding, response frequency.

Introduction

In light of revised extreme flood estimates around Australia, dam safety reviews have been carried out for a number of existing large dams that control spillway flows using radial gates. Hydraulic modelling of flows up to Probable Maximum Flood (PMF) has identified several spillways with the potential for the arms and trunnions of existing radial gates to be partially submerged by the peak flow.

Various upgrade solutions have been proposed to mitigate against this impact, for example at Wivenhoe Dam in Queensland a flat plate deflector was installed upstream of the radial gates to deflect flows away from the arms (Maher and Rodd 2005). More recently at Warragamba Dam and Wyangala Dam in NSW, a gate locking mechanism has been proposed to allow the gates to resist the additional hydrodynamic loading that the gates were originally not designed to withstand.

Wyangala spillway

Wyangala Dam is located on the Lachlan River near Cowra, approximately 200km west of Sydney. The 117m wide main spillway has a low ogee crest and is divided into eight gated bays (Figure 1). The spillway was originally designed for a peak outflow of 14,720m³/s (SMEC 2006). After revisions to the flood estimates, the current Dam Crest Flood (DCF) capacity is estimated at 18,000m³/s, corresponding to 1:9,000AEP. Proposed Stage 1 upgrade works aim to increase the outflow through the gates to 21,000 m³/s by raising the radial gates and a parapet wall crest raising, reducing the risk of DCF to 1:20,000 AEP.

Each radial gate is 14.63m wide and the radius from the trunnion hub to the skin plate of the gate leaf is 12.8m. The gate leaf is supported by the left and right gate arms, each consisting of three tapered I-section members (Figure 2).

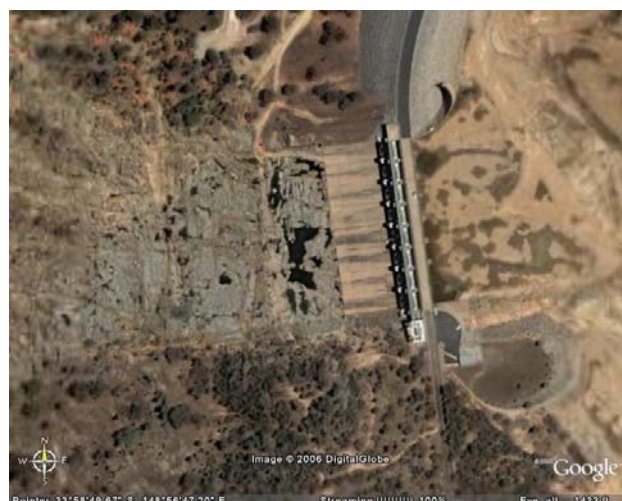


Figure 1: Aerial view of Wyangala Dam spillway (Source: Google Earth)

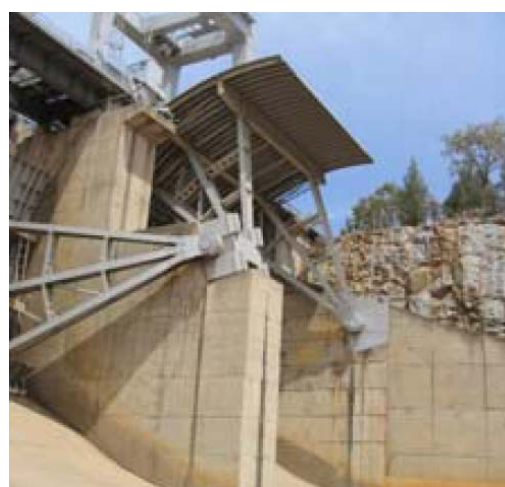


Figure 2: Photograph of Wyangala Dam spillway radial gates (Source: Hobbs 2007)

Several recent model studies have been carried out to examine the impact of the extreme flows. A 1:80 scale



Figure 3: Physical modelling of flow through gate arms (raised by 1.0m) at 21,000m³/s (SMEC 2006).

physical hydraulic model of the spillway was undertaken by SMEC in 2006. The model incorporated approximately 30Ha of upstream topography to ensure approach flows were correctly modelled. The model report (SMEC, 2006) and DVD video footage (SMEC 2006a, 2007) examined flow rates up to 22,000m³/s with the radial gates raised up to 2m higher than the original fully open position. For the case shown in Figure 3, with the gate raised by 1m above the fully open position, arm submergence of up to 5m was observed.

In 2008, WorleyParsons carried out a CFD study of the spillway to examine the hydrodynamic pressures on the raised radial gate arms, with the spillway discharging 21,000m³/s and the gates raised by an additional 1.4m above the original fully open position (WorleyParsons, 2008). The full model covered an area 200m upstream of the spillway crest and 180m either side of the spillway centreline, to capture the effects of the approach conditions on the individual bays.

Figure 4 shows the computed flow pattern at the spillway, overlaid by the raised radial gates, indicating submergence of up to 8m length of arm. For a detailed single-bay model, arm loadings were obtained using a simplified tapered rectangular beam model in place of the I-beam arm members. The computed time-varying loads did not indicate any dominant frequency of oscillation, however no validation of the model's ability to capture

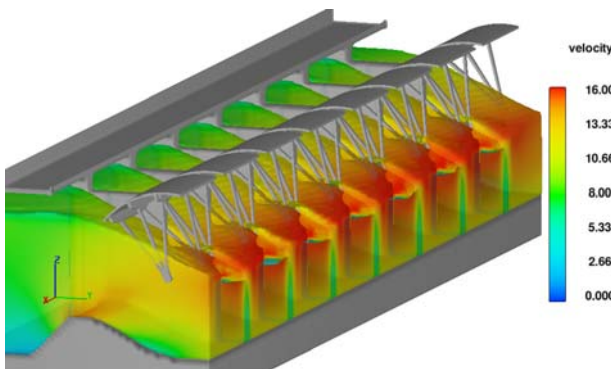


Figure 4: Computed flow surface superimposed on gates raised 1.4m (WorleyParsons, 2008)

this type of behaviour had been performed at the time, so it was not clear whether the lack of periodicity was real or a facet of the modelling.

In 2010, WorleyParsons was engaged by State Water Corporation to further examine whether flow excitation experienced by the submerged radial gate arms could cause resonance of the gate under DCF flows. The study comprised of four key tasks:

- Validate CFD modelling of vortex shedding behaviour
- Evaluate surface height fluctuations in spillway approach flow
- Detailed CFD modelling of fluid loads on a single gate
- FE response frequency study of radial gate

This paper will examine the key analysis and outcomes from each task.

Flow-induced vibration

When a member is submerged in a flow, it is subjected to a hydraulic loading where the mean loading is typically evaluated as a drag function. The fluctuating part of a loading on a member in flow can be the result of an extraneous source such as turbulence or a flow instability like vortex shedding. When the frequency of fluctuation in the flow is similar to the natural frequency of the member, destructive reinforcement of forces can occur.

Naudascher and Rockwell (1994) have examined in detail the various causes and effects of flow-induced vibration in the context of hydraulic structures. In the case of submerged radial gate arms, vibrations may be induced by upstream flow instabilities from the spillway approach geometry, or due to vortex shedding action generated at the submerged arms themselves. The present study examined the potential for both types of vibration, with a key focus on vortex shedding at the arm members.

Vortex shedding

Vortex shedding is an oscillatory flow separation pattern that can form when fluid flows past a blunt object such as a column or pier. Irregularities present in viscous flows result in a non-uniform low-pressure zone in the wake of the body, which gradually builds up to form alternate low-pressure vortices that periodically detach from the body and travel downstream (Figure 5).



Figure 5: Typical vortex shedding pattern

The differential pressures on the body result in an oscillating net force, where the frequency of oscillation is a function of the flow velocity, Reynolds number and

body size and shape, characterised by the Strouhal equation:

$$St = f D/V \quad (1)$$

where St = Strouhal number which is a function of Reynolds number and member shape; f = vortex shedding frequency (Hz); D = member width facing the flow (m); and V = approach velocity (m/s).

Vortex shedding behaviour results in periodic variations of the force components on the member. The lift force oscillates at the vortex-shedding frequency, while the drag force oscillates at twice the vortex shedding frequency (Sumer and Fredsøe, 2006).

If the frequency of vortex shedding is similar to the resonant frequency of the body, self-sustaining and potentially destructive vibrations can occur.

Vortex shedding validation data

A significant body of work has been generated by researchers trying to understand vortex shedding behaviour under different situations. The vast majority of this work relates to circular cylinders, using wind tunnel testing at relatively low Reynolds number (typically 10^2 to 10^5).

The present study focussed on flow conditions similar to those experienced by the Wyangala spillway radial gate arms during extreme flood, including:

- I-section member shape
- Non-zero angle of attack
- High Reynolds number flow (approx. 10^8)
- Nearby wall or pier
- Member inclined to the flow
- Supercritical flow ($Fr > 1.0$)
- Free surface

The following sections consider various published data applicable to these conditions.

I-section Strouhal number

An extensive literature search identified only one significant reference relevant to vortex shedding at I-beams. Grant and Barnes (1981) assessed the drag coefficient and Strouhal number of an I-beam for various angles of attack. Figure 6 shows the Strouhal number varying between 0.11 and 0.19 depending on the orientation of the member to the flow. The result is approximately symmetrical about an angle of 90° as expected, with maximum peaks at 20° and 160° angles of attack, and minimum at 90° .

Other more general references found include *Hydrodynamics Around Cylindrical Structures* by Sumer and Fredsøe (2006) which provides an excellent summary of the state of the research up until 2006, and *Dynamics of Fixed Marine Structures* by Barltrop and Adams (1991) which provide Strouhal numbers for different I-beam cross section shapes ($B/D = 1.0, 0.5$ and

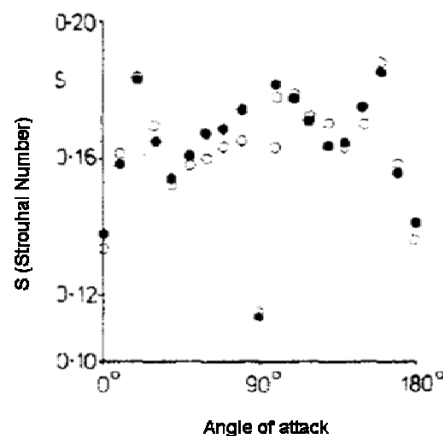


Figure 6 Comparison of I-section Strouhal number for high Reynolds number and various angle of attack. (Reproduced from Grant and Barnes, 1981).

0.25). The Strouhal numbers in these two references concur with those from Grant and Barnes.

For the CFD validation study, a Strouhal number of 0.14 was used for comparison with the CFD model for cases where the angle of attack is 0° .

Reynolds number effects

Sumer and Fredsøe report that for large Reynolds numbers ($>10^5$) the vortex shedding frequency is relatively constant for members with fixed points of flow separation such as sharp-edged sections. This is in contrast to circular members which undergo a number of flow transformations as Reynolds number varies.

Wall effects

Sumer and Fredsøe also discuss the effects of nearby walls, but only for circular sections. When a circular cylinder of diameter D is placed near a wall:

- Vortex shedding is suppressed for gaps less than $0.3D$
- The vortex shedding frequency may increase very slightly (up to 10%) for gaps less than $2.0D$
- The drag force is reduced by up to 50% for gaps less than $1.0D$
- The mean lift force becomes non-zero for gaps less than $0.5D$

At the outer bays of Wyangala spillway, the gap between the full-height training wall and the arm members for the raised radial gate varies between $1.2D$ near the hub and $2.8D$ near the gate leaf (where D is the width of the web section). Assuming similar behaviour of circular and I-beam cross-sections (which may not be the case), this data suggested that the presence of the wall would not significantly affect vortex shedding behaviour.

Where the radial gate arms are adjacent to a concrete pier, a more complex scenario occurs due to the cut-out section (see Figure 2) above the trunnion level. When the gates are raised, the arms will be adjacent to the pier wall only at localised areas near the hub and gate leaf. No validation data was found for this kind of complex scenario.

Inclined member effects

Sumer and Fredsøe describe the effect when a circular cylinder is inclined to the flow. Observed streamlines have shown that although the approaching flow is at an angle, the streamlines in the neighbourhood of the member are bent in such a way that the actual flow is at an angle of about 90° (Figure 7). For inclinations tested up to 45°, the vortex shedding frequency was found to be independent of the angle of incidence when calculated using the velocity component *normal* to the member, implying that Equation 1 adjusts to:

$$S_t = f D / V \cos(\alpha) \quad (2)$$

where $V \cos(\alpha)$ is the velocity component normal to the member; and α is the angle of inclination to the flow.

Sumer and Fredsøe note that this relationship is thought to break down when the angle of incidence is greater than 55°, because the streamlines no longer bend. Lucor and Karniadakis (2004) noted a reduction in vortex shedding energy for angles greater than 60°. However, it is uncertain how the findings above would apply to a non-circular bluff body.

For the Wyangala gate arms, the angle of inclination to the flow can be up to 60°. Using Equation 2, the vortex shedding frequency may be reduced by up to 50% compared to a member that is perpendicular to the flow.

Supercritical flow and free surface effects

No references could be found that describe the effects of supercritical flow (Froude no. > 1.0) or situations where the member protrudes through the free surface during supercritical flow. These effects were unable to be

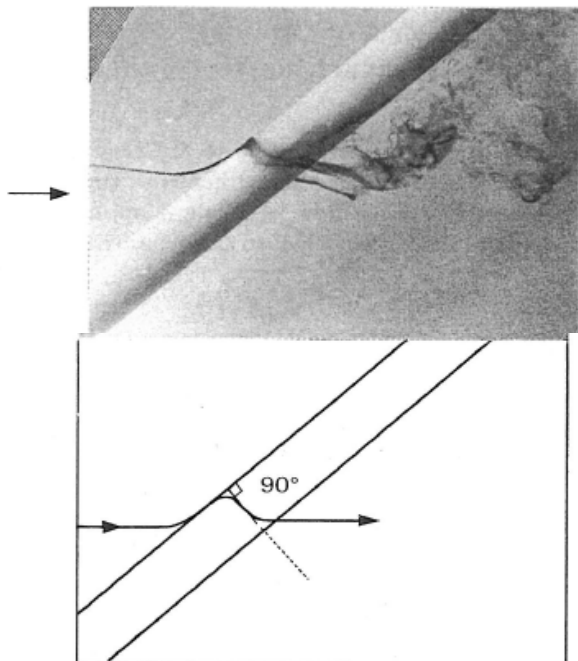


Figure 7: Visualisation of flow past an inclined circular cylinder. (Reproduced from Sumer and Fredsøe, 2006).

validated against published data.

CFD validation study

The objective of the CFD validation study was to prove the validity of the CFD code in correctly capturing the vortex shedding behaviour as water flows past a submerged body, and systematically examine those effects for which no validation data was available.

The CFD modelling was carried out using the general-purpose commercial software FLOW-3D Version 9.4.

Methodology

The ability of the CFD software to accurately capture the vortex shedding behaviour around an I-section was examined using a series of 2D and 3D CFD analyses. Starting with a simple fully-submerged 2D model, each successive model added further complexity to the analysis, up to the final 3D model which was representative of the actual flow conditions at the Wyangala radial gate during extreme flood. The parameters examined included effects from the free surface, adjacent wall, non-zero angle of attack, inclined member and supercritical flow conditions.

For each analysis case, the force time histories (lift and drag) were extracted once the analysis reached a ‘steady-state’ flow (where vortex shedding occurred, this was a ‘dynamic steady-state’). A data sampling rate of 250Hz was used to ensure capture of higher frequency vibrations up to 30Hz. A Discrete Fourier Transform analysis was carried out on the time-history data to identify any significant frequencies of vibration.

Where possible, the computed results were compared against theoretical values and qualitative expected outcomes identified from published data.

Model setup

A 2D model of an I-beam was set up with the dimensions based on the lower arm beam of the Wyangala Dam radial gates which has a constant flange width (B) and variable web width (D). The selected D/B ratio was 1:0.67, which corresponds to that used in the experiments of Grant and Barnes and is representative of the Wyangala gate arm at a distance of 6.2m from the hub. The modelled dimensions are shown in Figure 8, and Figure 9 shows the CFD model geometry and initial mesh grid.

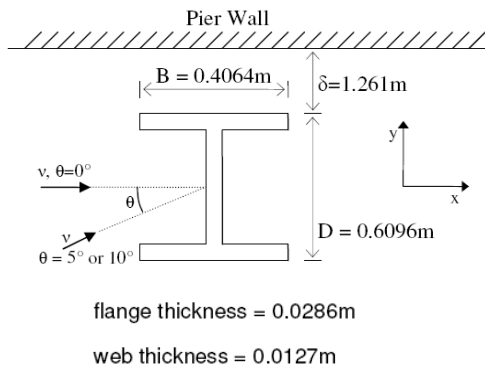


Figure 8: Model geometry (not to scale)

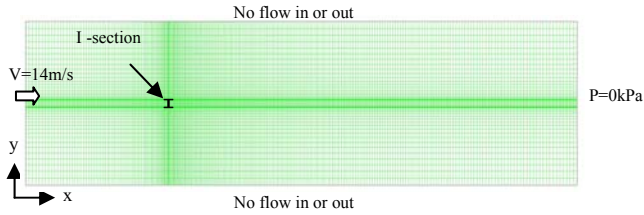


Figure 9: 2D model mesh and boundary conditions

A flow velocity of 14m/s was selected for analysis, based on the typical velocity near the gate arms computed in the previous CFD study (WorleyParsons, 2008). For the cases where a free surface was modelled a flow depth of 20m was required to ensure uniform (critical) flow and prevent variations in the flow velocity due to accelerations.

Validation results

A total of fifteen validation analysis cases were carried out during the study. Findings for the key cases of interest are described below.

2D fully submerged model

The simplest case undertaken was a 2D model with a 0° angle of attack. This model successfully generated a vortex shedding behaviour, with the fluctuating lift and drag forces developing over approximately 12s, after which a regular fluctuating forcing frequency was achieved. The computed fluctuating lift and drag frequencies (3.5 Hz and 7.1 Hz) were within 10% of the theoretical values (3.2Hz and 6.4 Hz) for the modelled condition.

Figure 10 shows the vortex shedding behaviour for three 2D models, showing the effect of angle of attack and the presence of a pier wall. Typical vortex shedding behaviour is seen in each case.

The computed Strouhal numbers are compared graphically to Grant and Barnes' angle of attack data in Figure 11, showing good agreement. The wall and the flow angle did not have a significant impact on the computed vortex shedding frequencies.

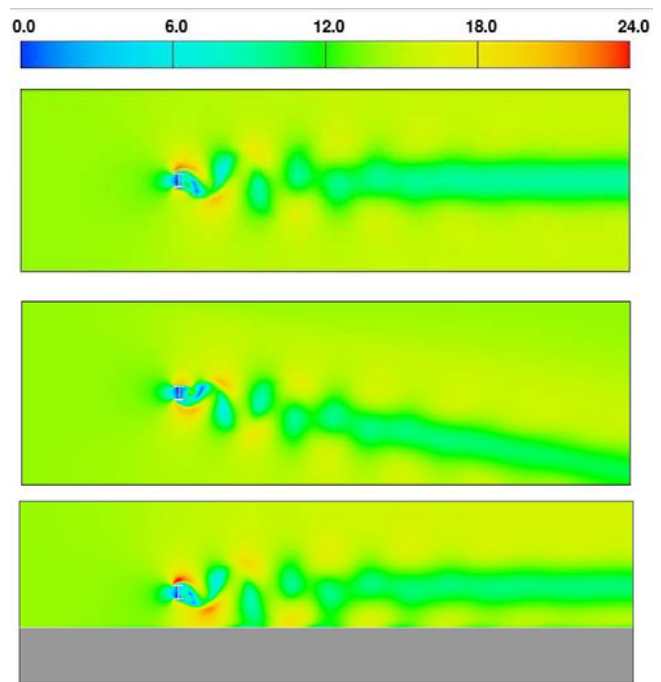


Figure 10: Velocity (m/s) contour plot showing vortex shedding downstream of I-section: (top) flow normal to I-section; (middle) flow at 10 degrees to I-section (bottom) with wall

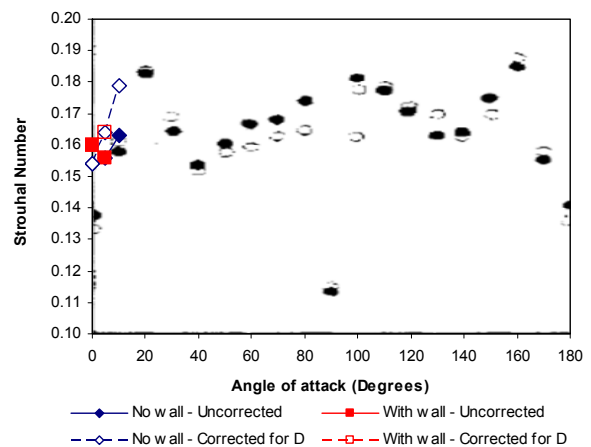


Figure 11: Overlay of 2D results on Grant and Barnes data

3D fully submerged model

The addition of depth to the model resulted in the formation of additional vorticity in the third dimension. For the simple case with 0° angle of attack, Figure 12 shows a 3D visualisation of the vortices. The main z-axis vortices show clearly (coloured light blue and green), while minor alternately-rotating x-axis vortices (shown in dark red and purple) also appear in the 3D model. The frequency of vortex shedding in the lift and drag were very similar to the 2D models, as expected.

Several fully submerged 3D models were also undertaken with the member inclined at 60° to the flow. These models showed a complex flow pattern in the

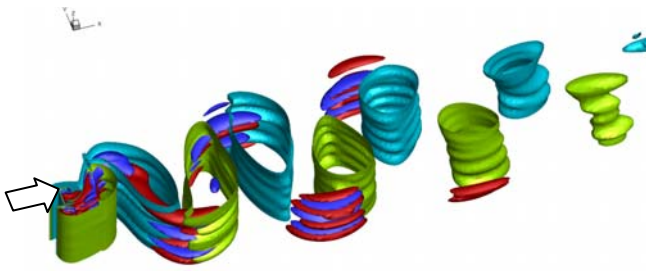


Figure 12: Visualisation of 3D vorticity about the z-axis (green/blue) and the x-axis (red/purple). Arrow indicates direction of flow.

region downstream of the I-beam. There were significant end effects at the top and bottom of the model, which resulted in the flow no longer showing the quasi-2D flow patterns seen for the previous 3D models. Instead, a strong primary vortex formed behind the I-beam, which flattened towards the bottom of the model and detached only in this localised area. This behaviour is represented in Figure 13 using streamlines. In addition, the shedding behaviour changed from asymmetrical to symmetrical, and varied significantly in frequency and magnitude depending on the length of member modelled. The streamlines travel normal to the member in some locations, similar to the behaviour described by Sumer and Fredsøe.

Without further detailed study of the flow patterns, and proper validation, it is difficult to apply much significance to the present set of results obtained for the inclined member under submerged flow. These represent special cases where the method of modelling the member apparently did not represent an idealised theoretical case. It is considered that the results obtained for the inclined member are unrepresentative of real conditions.

Ideally, some additional testing with smaller angles of inclination and greater water depth to minimise end effects could be carried out to identify the trend in the model, however this could require significant research effort which was beyond the scope of the current project.

3D model with free surface

When the free surface was introduced to the model, a void formed on the downstream side of the I-section (Figure 14), reflecting the region of low pressure seen behind the I-section in the 2D and 3D submerged models. The void extended approximately 5.5m below the upstream surface.

From the published literature, it was not certain whether vortex shedding should be seen in the submerged region below a supercritical free surface. The cross section plots in Figure 15 and 16 show a complex flow pattern, but no coherent vortex shedding pattern. This may be a result of the large variation in water levels behind the member.

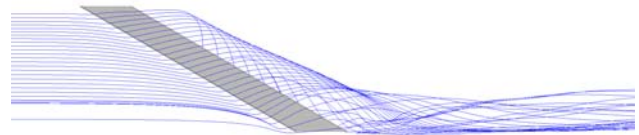


Figure 13: Streamlines showing vortex formation around inclined I-section

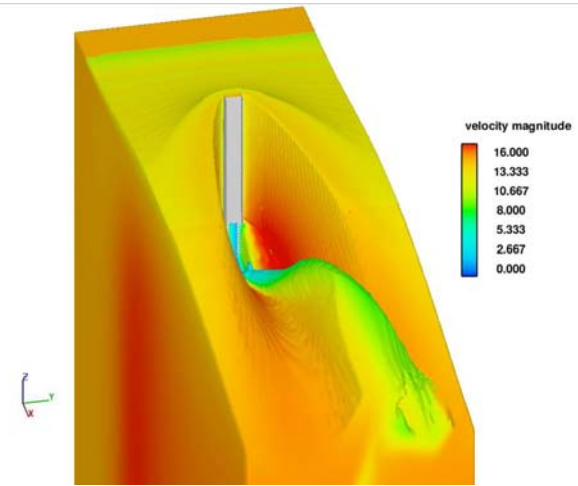


Figure 14: Velocity contour plot showing flow splitting downstream of I-section with free surface (m/s)

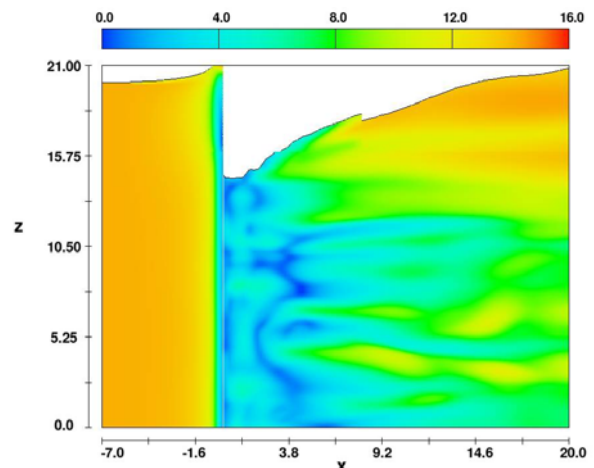


Figure 15: Long-section through centreline of Figure 14, coloured by velocity (m/s)

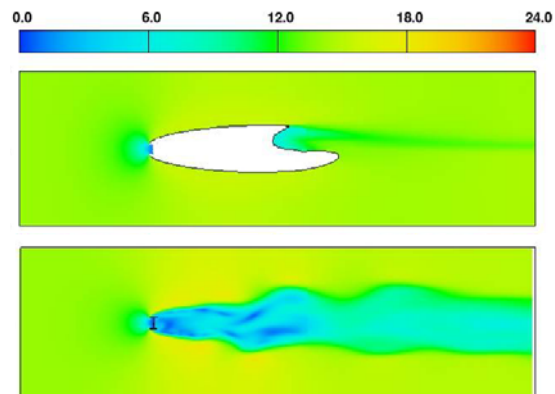


Figure 16: Cross-sections through void (top) and submerged region (bottom), coloured by velocity (m/s)

The computed lift and drag forces showed no evidence of vortex shedding, either in the upper region where the flow splits, or in the lower submerged region.

Approach flow instabilities

The full spillway CFD model was analysed for 21,000 m³/s discharge and the water level at various locations around the model was extracted over time to determine whether regular fluctuations were occurring in the spillway approach flows that could lead to gate excitation.

Assessment of surface height fluctuations in the CFD model suggested approach flow variations in the order of 0.2 to 1.0Hz.

Surface height fluctuations recorded in the physical model video footage were also examined. By estimating the period between wave peaks, generally long-period (10 to 20 seconds) waves were observed in the approach flow. Some of these longer-period waves may have been due to reflections at the sides of the physical model, particularly in shallower regions, however the large upstream extent of the model helped to minimise any effects of laboratory conditions. Unfortunately, due to the time scale factor (1:8.94) of the physical model and the video frame rate (25fps), the maximum frequency that could be observed in the video was ~0.6Hz.

The two models suggested that approach flow height variability typically involved relatively long-period waves with frequencies less than 1 Hz.

Detailed CFD analysis of gate loadings

Based on the full spillway CFD model results (Figure 17), a more detailed sub-model of a single bay was analysed. The detailed model applied the computed time-averaged velocities from the larger model of the upstream boundaries to ensure the approach flow angle and velocity distribution was captured. Side boundary flows were also applied from the larger model to allow for incoming flows from adjacent bays across the back of the pier. The upstream boundary was located beyond the nose of the pier to allow generation of bow wave effects.

The raised gate arms were included in this detailed CFD model and the upstream flow conditions were transferred from the full spillway model results.

Due to the high mesh resolution required to accurately model the flanges of the I-sections, the left and right arms were examined in two separate models where one arm was modelled with a detailed geometry and mesh, and the other arm was idealised as a set of rectangular blocks. At the left arm, the flow was permitted to spread laterally at the concrete pier cut-out, while at the right arm the full-height training wall was modelled.

The sub-models were analysed for a period of 20 seconds, which previous models have shown was sufficient time to allow development of vortex shedding behaviour. The flow patterns and arm loads were extracted from the sub-models and the forcing frequencies experienced by the arms were estimated using Fourier Transform methods.

General behaviour

The flow surface is plotted in Figure 18 for the right gate arm. The lower member splits the free surface, creating a void on the downstream side of the member and providing significant shielding to the middle and top members. These two members have some impact from flows that reflect from the side wall and become caught up in the upstream cavity of the I-section, as shown in the horizontal cross-sections at Figure 19.

Figure 20 shows the extent of submergence of each member of the right gate arm. The bottom member was found to be fully submerged over a length of 2.8m, with an additional 5.4m length partially submerged. The top member did not become fully submerged at any point.

The left arm showed similar patterns, with a lower level of submergence due to asymmetry in the approach flows to the bay. Flows entering behind the pier from the adjacent bay (applied based on the computed flow patterns from the full model) formed a ‘rooster tail’ effect behind the pier, but had limited impact on the left arm members.

Vortex shedding potential

The validation analysis showed that for supercritical free surface flows, vortex shedding is only possible in areas where the member is fully submerged, and may not occur even in these locations. The detailed CFD analysis of the gate arms showed that the bottom member is fully submerged over a length of two to three metres. In the submerged area between the lower and middle members, there is a maximum distance of only one metre (approx. 2.5D) within which vortices could form. This limitation, combined with the member inclination and complex free surface, makes it unlikely that any coherent disturbance could occur.

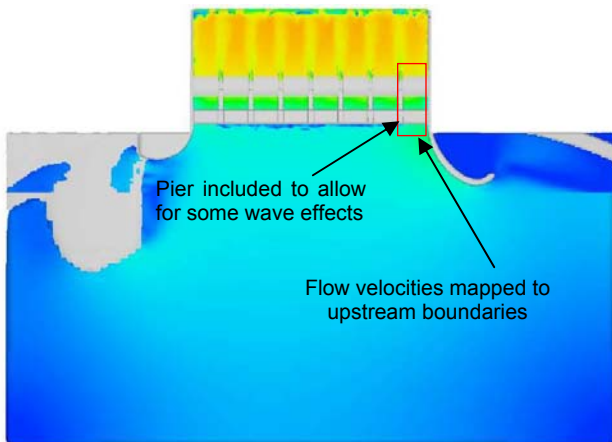


Figure 17: Plan view of full spillway CFD model geometry including topography and spillway, and extent of single bay sub-model.

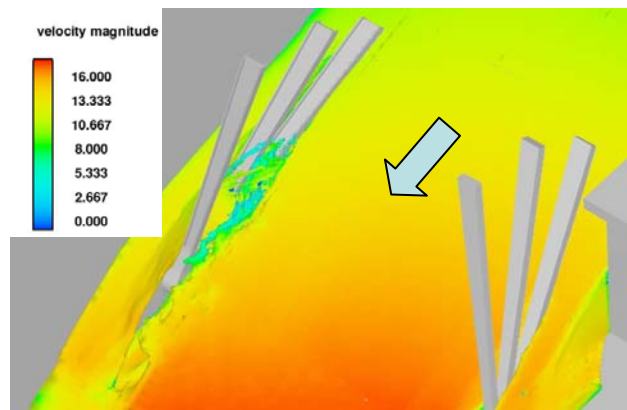


Figure 18: Isometric view of the flow pattern around right gate arm. Arrow shows direction of flow.

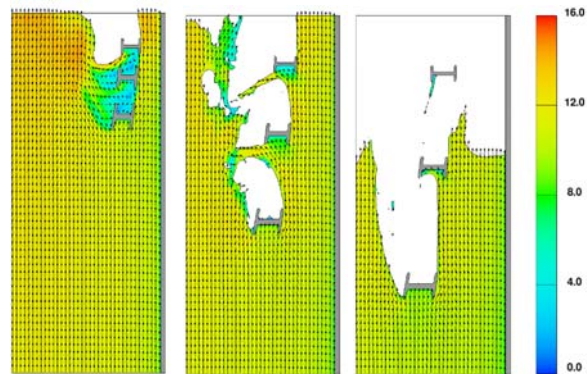


Figure 19: Flow patterns around right gate arm at three elevations, coloured by velocity (m/s).

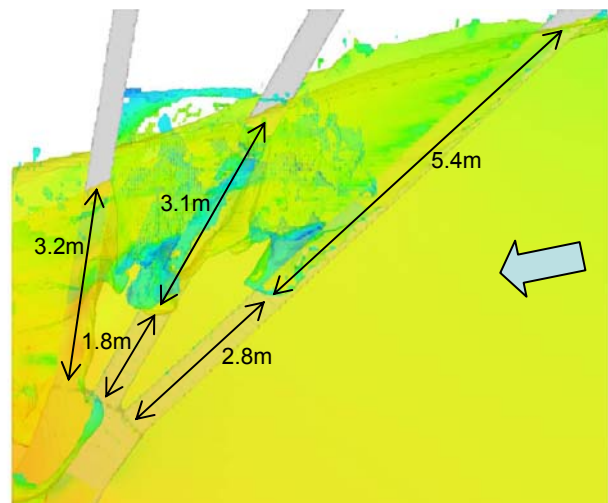


Figure 20: Elevation view of right gate arm members. Water surface is semi-transparent to show extent of arm submergence (full and partial).

The member force time-history (Figure 21) shows a lot of noise and Fourier analysis of the data results in a very flat power spectrum with no dominant frequencies (Figure 22).

Gate response study

An existing finite element of the Wyangala Dam radial gate, originally generated by the Department of Commerce using Strand7, formed the basis of this study. This model was used to investigate the natural frequency of the system with a focus on a proposed locking mechanism and the effect that this may have on the vibrational behaviour of the gate arms.

A conceptual locking mechanism, developed by MWH (2009), was incorporated into the Strand7 model.

A series of linear elastic eigenvector analyses were carried out to determine the mode shapes and frequencies for different scenarios with various edge fixities and stiffening of the radial gate.

Table 1 lists four key modes identified by the analysis. The first is for the gate in its current form without modification and heavily involved the gate arms with a sway and twist movement and fundamental frequency of 2 Hz (Figure 23 left).

Application of the locking mechanism allowed a swaying motion of the gate, heavily involving the arms at a frequency of approximately 5 Hz (Figure 23 right). With

additional lateral fixing of the three horizontal girders this mode was eliminated.

The next mode of interest, at approximately 11 Hz, proved to be a function of the overall gate construction and the limit to which girder fixity could prevent vibration of the system (Figure 24 left). Further stiffening of the skin plate structure increased the fundamental model to 13 Hz (Figure 24 right).

Table 1: Key gate mode shapes and frequencies

Frequency	Gate configuration	Mode shape
2.0 Hz	Existing gate	Gate arm sway and twist movement
5.0 Hz	Proposed locking mechanism	Gate arm sway movement
11 Hz	Proposed locking mechanism, lateral fixity on all three horizontal girders	Primarily involves skin plate - minor radial arm movement
13 Hz	Proposed locking mechanism, lateral fixity on all three girders, skin plate stiffening	Gate arm sway and skin plate twist

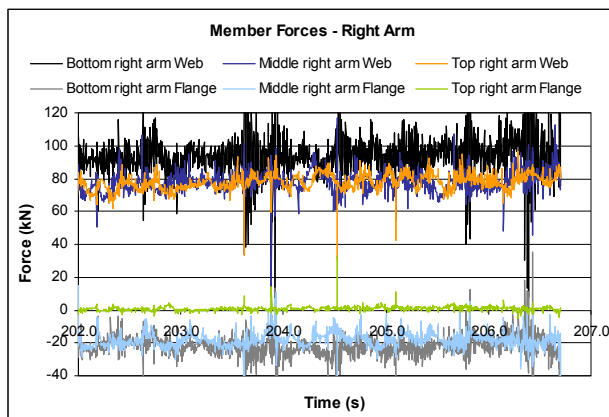


Figure 21: Time-history trace of arm member forces, right arm.

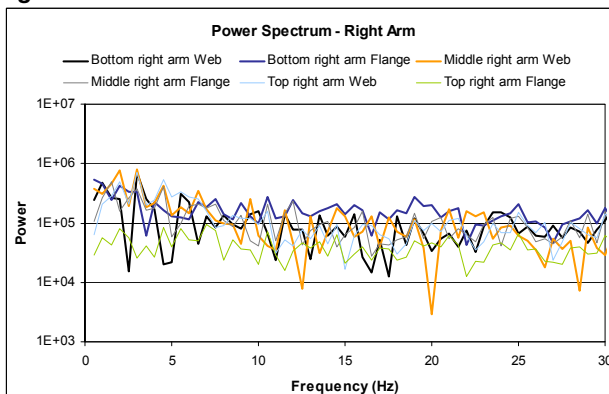


Figure 22: Fourier analysis power spectrum, right arm

Discussions and conclusions

Validation study

The main objective of the validation study was to confirm the ability of CFD to model vortex shedding with an accurate computation of the vortex shedding frequency, under flow conditions similar to those occurring at

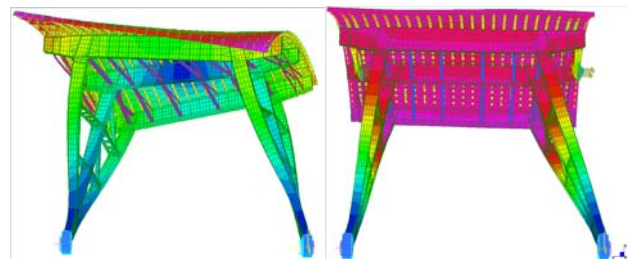


Figure 23: left: Existing gate (2.0Hz); right: with locking (5.0 Hz);

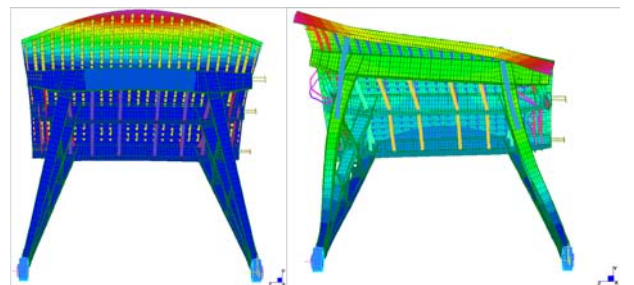


Figure 24: left: Full girder fixity (11 Hz); right: additional skin plate strengthening (13 Hz);

Wyangala Dam spillway during extreme outflows. This has been shown to be possible for simple 2D and 3D cases, with and without the presence of a full height side wall, and for varying low angles of attack. Typical frequencies of 3.5 and 7Hz were achieved for the fluctuating lift and drag forces, respectively.

With the addition of more realistic parameters like the 60° member inclination and a free surface, the flow behaviour became considerably more complex and vortex shedding behaviour differed markedly from the previous simple cases. Unfortunately due to the lack of published data describing these effects, these results could not be fully validated.

For the case when the submerged member is inclined to the flow, the results were inconclusive, with end effects appearing to suppress or magnify the vortex shedding effects depending on the modelled length of the member.

For supercritical free surface flows, the I-beam section causes splitting of the flow around the beam, with a void forming in the lee of the beam. Under this situation, vortex shedding ceases. This behaviour seems reasonable. At the lower portion of the beam, the void may close up – in this submerged region, localised vortex shedding may potentially occur but was not seen in the test models.

Approach flow instabilities

Assessment of surface height fluctuations in the CFD model and from the physical model video footage (21,000m³/s flood case) suggested that approach flow variations are typically long-wavelength with frequencies less than 1.0Hz.

Detailed arm model

The hydrodynamic forces from the highly turbulent and supercritical flow acting on the raised radial gate lower arms were predominately due to flow splitting/momentum transfer mechanism with a small amount of drag near the trunnion region. At the right side, the middle and upper arms were impacted by water channelled along the training wall. The lower arm members act to shield the middle and upper arm members from the main flow.

Fourier analysis of the computed arm force time histories showed no dominant frequency of vibration. The highest peaks were below 3Hz, but even these were of limited significance.

Structural response

Linear elastic eigenvalue extraction analysis of the gate structure identified a range of mode shapes and frequencies, which were dependent on the level of fixity. With no lateral restraint or locking brakes, the fundamental frequency was found to be 2Hz. With the locking brakes engaged and lateral restraints provided at

the ends of the girders, the first mode of vibration was at a frequency of just over 11Hz. The fundamental frequency was difficult to increase above this value without further modifications to the gate structure.

Potential for flow-induced vibration

Based on the analyses carried out, flow-induced vibration of the radial gate with the braking mechanism and lateral fixity engaged appears unlikely. The calculated frequency of approach flow instabilities was less than 1Hz - well away from resonant frequencies of the locked gate. The detailed modelling of the gate arms suggested that vortex shedding behaviour is unlikely to occur.

In view of the potential uncertainty associated with the CFD modelling, a separate assessment using the Strouhal equation was performed to check if the gate will undergo resonance assuming vortex shedding behaviour was occurring at the submerged arms. Considering the potential variability of the flow velocity, submerged arm width, Strouhal number (from published values) and member inclination, Figure 24 shows that the vortex shedding frequency could range between 1Hz and 7Hz

A conservative approach would require the adopted gate locking solution to ensure the resulting fundamental frequency of the gate exceeds 11 Hz.

Limitations and recommended further study

CFD modeling of detailed member geometries is still limited by computational power. The present 3D detailed analysis of a single radial gate required up to a week of runtime to examine a 20-second time-history. Ideally, a much longer time-history would be desirable.

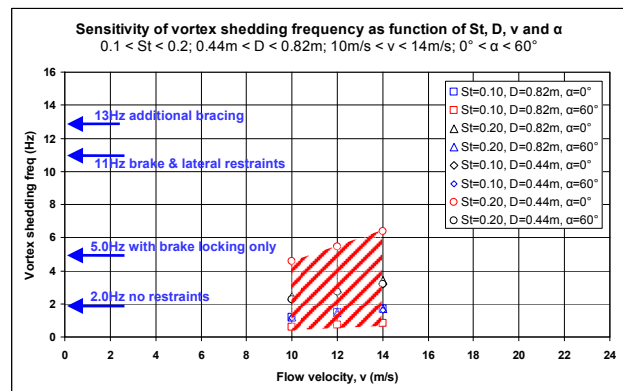


Figure 25: Assessment of the vortex shedding frequency using the Strouhal number equation.

The validation study was restricted by the limited data available for comparison. There is a lack of published experimental data for non-circular cylinders, particularly at high Reynolds numbers and with free surface conditions at critical and supercritical flows. Additional large scale physical model studies of relevant cases are recommended to provide greater certainty, and also allow

improved validation of numerical models for these flow conditions.

Acknowledgements

The authors gratefully acknowledge State Water Corporation, Brian Cooper, MWH and WorleyParsons for their support for the work underlying this paper.

References

- N.D.P. Barltrop and A.J.Adams (1991) *Dynamics of Fixed Marine Structures*, Third Edition, The Marine Technology Directorate Limited, Butterworth Heinemann, Oxford, UK.
- I. Grant and F.H. Barnes (1981) "The Vortex Shedding and Drag Associated with Structural Elements". *Journal of Wind Engineering and Industrial Aerodynamics* 8, 115-122
- Glen Hobbs and Associates (2007) Wyangala Dam Radial Gates Investigation Raising the Gates Final Report Contract No 3754.
- B Maher and R. Rodd (2005) 'Wivenhoe Alliance – Investigation to pursue innovation', *Proceedings, 45th ANCOLD Conference*, Fremantle WA.
- W Naudascher and D Rockwell (1994) *Flow-Induced Vibrations An Engineering Guide*. Dover Publication. USA.
- MWH (2009) Wyangala Dam Flood Security Upgrade Detailed Concept Design for Gate Raising and Loading System Contract No 4044. Design Report. (11 Dec 2009)
- SMEC (2006) Physical Model Study for Wyangala Dam Spillway Separable Portion 1 – Contract No 3672 Final Report.
- SMEC (2006a) Wyangala Dam Spillway Model Study – Contract 3672. Final DVD Presentation Separable Portion 1, 12 Oct 2006.
- SMEC (2007) Wyangala Dam Spillway Testing – Additional Tests with Gates Raised above Normal Fully Open Position. DVD Jan 2007.
- B.M. Sumer and J. Fredsøe (2006). *Hydrodynamics around Cylindrical Structures*. World Scientific Publishing. Singapore.
- WorleyParsons (2008) Wyangala Spillway CFD Study. Report No. 301015-00292-RP001, 28-Oct-2008